Acta Cryst. (1957). **10**, 629

The Effect of Crystal Shape and Setting on Secondary Extinction*

By Walter C. Hamilton

Chemistry Department, Brookhaven National Laboratory, Upton, Long Island, New York, U.S.A.

(*Received* 17 *December* 1956 *and in revised form* 20 *April* 1957)

The power equations for diffraction from a single crystal of uniform, but arbitrary, cross-section may be solved by numerical procedures to yield secondary extinction coefficients. Calculations are carried out and curves are presented for both absorbing and non-absorbing crystals of circular and rectangular cross-section at several crystal settings and Bragg angles. It is shown that the extinction coefficient for crystals of rectangular cross-section can be quite sensitive to the direction of the incident beam relative to the crystal faces; hence, if extinction is severe, the use of a cylindrical crystal is indicated. In the cylindrical crystal, the extinction coefficient becomes noticeably dependent on the Bragg angle as the extinction becomes more severe. A single-parameter empirical extinction correction of the exponential or linear type commonly used cannot then be valid for groups of reflections which vary widely in Bragg angle. Only if $I_o/I_c > 0{\cdot}70$ is an extinction coefficient of the type exp $(-kI_c)$ appropriate. An estimate of the mosaic spread parameter may thus be obtained from the less severely extinguished reflections and applied to the more intense reflections. The mosaic-spread parameter may also be conveniently estimated from the limiting intensity if this is experimentally observed.

Introduction

The problem of secondary extinction in diffraction experiments has been treated by several authors. (See, for example, Zachariasen (1945), Bacon & Lowde (1948), and James (1950).) These authors have generally confined their theoretical treatments to infinite flat plates and their empirical corrections to one-parameter functions. Because of the increasing use in structure refinements of very accurate intensity measurements on single crystals, it seems of interest to examine the effect of crystal shape on the secondary extinction coefficient. This is of particular importance in neutron-diffraction studies, where corrections for secondary extinction are generally far more important than those for absorption. The reverse is true for X-rays.

Theoretical

We shall consider a crystal which has uniform cross-section in planes parallel to the plane defined by the incident and diffracted beams, the axis of crystal rotation being taken perpendicular to these planes†. We shall further specify that the boundary curve of the cross-section be convex, i.e., there are no possible points of re-entry for an emergent beam. Let us define a Cartesian co-ordinate system (rectangular only if $2\theta = 90°$) with an axis **n** parallel to the incident beam and an axis **m** parallel to the diffracted beam. The angle between the axes is 2θ (see Fig. 1).

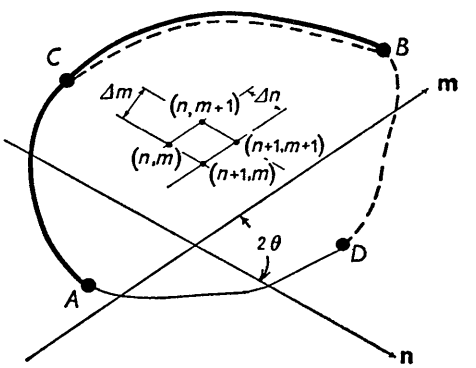

Fig. 1. Cross-section of arbitrarily shaped crystal specimen showing coordinate grid and axes parallel to incident and diffracted beams. Heavy full line: entry surface; heavy broken line: exit surface.

Generalizing the formulae of Zachariasen (1945), we may write

$$\left.\begin{aligned}\partial P_H/\partial m &= -(\mu+\sigma)P_H+\sigma P_0 \equiv \tau P_H+\sigma P_0\,,\\ \partial P_0/\partial n &= -(\mu+\sigma)P_0+\sigma P_H \equiv \tau P_0+\sigma P_H\,,\end{aligned}\right\} \quad (1)$$

where

P_0 = power per unit area in primary beam at the point (n, m),
P_H = power per unit area in diffracted beam at the point (n, m),
μ = linear coefficient of true absorption,
σ = $Q'W(\Delta\theta)$,
Q' = QE_p with E_p a correction for primary extinction, with which we are not concerned,
Q = $\left(\frac{\lambda^3 F^2}{V_c^2 \sin 2\theta}\right) cm^{-1}$ for equatorial reflections (neutrons),

* Research carried out under the auspices of the U.S. Atomic Energy Commission.

† The extension to crystals of non-uniform cross-section is straightforward, involving integration of the intensity along a direction perpendicular to the sections. In the present treatment, this is accomplished merely by multiplying the result for a single section by h, the height of the crystal.

$Q = \left(\frac{e^2}{mc^2}\right)^2 \frac{(1+\cos^2 2\theta)\lambda^3 F^2}{2V_c^2 \sin 2\theta}$ cm^{-1} for equatorial reflections (X-rays),

V_c = unit cell volume,

λ = wavelength of neutrons or X-rays,

$W(\Delta\theta)$ = distribution function for mosaic blocks in terms of $\Delta\theta$, the deviation of a mosaic block from the mean Bragg angle θ;

e, m, c, and F^2 have the usual meanings, τ is defined as $-(\mu+\sigma)$ and is always negative. The differential equations are to be solved under the following boundary conditions:

$$\left.\begin{aligned} P_0 &= P_0^\circ \text{ along } ACB, \text{ the surface of incidence,} \\ P_H &= 0 \quad \text{along } DAC, \text{ the surface opposite the surface of emergence of the diffracted beam.} \end{aligned}\right\} \quad (2)$$

The integrated intensity for the rotating-crystal method is then given by

$$R^\theta = \frac{h\int_{-\infty}^{+\infty} d(\Delta\theta)\int_{nC}^{nD} dn \sin 2\theta P_H(n_s, m_s)}{P_0^\circ \int_{-\infty}^{\infty} W(\Delta\theta)d(\Delta\theta)}, \quad (3)$$

with $P_H(n_s, m_s)$ being the value of P_H along the surface s of the crystal defined by CBD. h is the height of the crystal. P_H is of course a function of $\Delta\theta$ as well as of m and n; hence the integration over $\Delta\theta$. The integral in the denominator of (3) will be unity, as distribution functions are usually so normalized. The factor $\sin 2\theta$ occurs because of the obliqueness of the coordinate system and the fact that the power is defined per unit area *perpendicular to the direction of propagation*. $\sin 2\theta dn$ is an infinitesimal length perpendicular to **m**, the direction of P_H. For $2\theta = 0°$ or $180°$, $\sin 2\theta dn$ must be replaced by the appropriate differential.

In general, the differential equations (1) will be difficult to solve. An iterative procedure could be used, but the boundary conditions for crystals with other than very simple shapes (parallelepipeds with faces parallel to **n** and **m**) cause this method to rapidly become unmanageable. It seems that numerical integration would be both general and practical. With this in mind, we may replace the equations (1) by the following difference equations

$$\left.\begin{aligned} P_H(n, m) &= P_H(n, m-1)[1+\tau\Delta m] \\ &\quad + P_0(n, m-1)\sigma\Delta m, \\ P_0(n, m) &= P_0(n-1, m)[1+\tau\Delta n] \\ &\quad + P_H(n-1, m)\sigma\Delta n, \end{aligned}\right\} \quad (4)$$

where P_H and P_0 are the values of the power arriving in the parallelogram denoted by the point (n, m) on a grid of mesh size $\Delta n \times \Delta m$ (see Fig. 1). Starting from the points of the grid near the boundaries ACB and DAC, we may use equations (4) to determine the values of P_H and P_0 at all points of the grid*. In particular, we are interested in the values of P_H at the first points of the grid outside the boundary CBD. If we let these values be denoted $P_H(a)$, $P_H(b)$, ..., $P_H(k)$, the integrated intensity becomes

$$R^\theta = h\int_{-\infty}^{+\infty} R(\Delta\theta)d(\Delta\theta) \Big/ \int_{-\infty}^{+\infty} W(\Delta\theta)d(\Delta\theta), \quad (5)$$

where

$$R(\Delta\theta) = \left[\frac{P_H(a)+P_H(k)}{2} + \sum_{i=b}^{k-1} P_H(i)\right]\Delta n \sin 2\theta\dagger. \quad (6)$$

It is generally assumed that $W(\Delta\theta)$ is a Gaussian distribution function with standard deviation η, termed the mosaic spread parameter. However, it will be convenient here to adopt a simpler form for $W(\Delta\theta)$ as follows:

$$W(\Delta\theta) = \begin{cases} 1/2\eta/3 & \text{if } |\Delta\theta| \le \eta/3 \\ 0 & \text{if } |\Delta\theta| > \eta/3 . \end{cases} \quad (7)$$

For such a distribution function, the integrated intensity is given simply by

$$R^\theta = h2\eta/3[R(\Delta\theta)]_{\Delta\theta=0}, \quad (8)$$

and the integration over $\Delta\theta$ in equation (5) is no longer necessary. The effect of this change in the form of $W(\Delta\theta)$ will be discussed in the Appendix.

We will define a secondary extinction coefficient by

$$E_s = R^\theta/Q'VA, \quad (9)$$

where V is the volume of the crystal and A is a pure absorption factor.

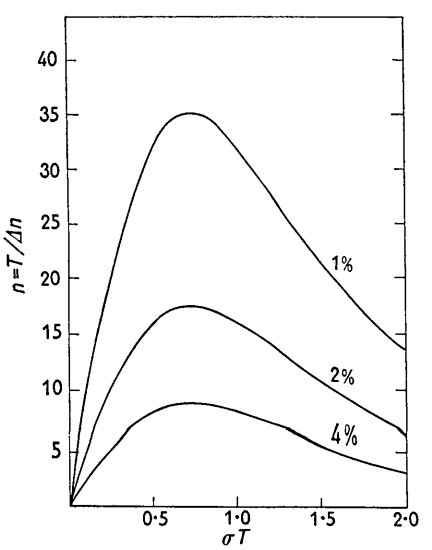

Fig. 2. Mesh size necessary for indicated error in secondary extinction coefficient. Flat plate of thickness T at $2\theta = 0°$.

* An analog computer would be especially suited to this problem.

† Other quadrature formulae might well be more suitable in a particular case. The trapezoidal formula is chosen here for simplicity in illustration.

It is important in performing the integrations to choose a mesh size small enough to obtain the desired accuracy in E_s. As a guide to the approximate size necessary, Fig. 2 shows $n = T/\Delta n$, the number of subdivisions necessary to obtain E_s with a given percentage error for a flat plate of thickness T at a Bragg angle of 0°. It will be noted that a very coarse mesh can be tolerated if one is willing to accept an error as great as 5%—a level which is often comparable to the error introduced in experimental estimation of the intensities. Alternatively, one may perform the calculation for three or more values of Δn and extrapolate to $\Delta n = 0$.

Limiting cases

For angles $2\theta = 0°$ or 180°, in which cases the directions of **m** and **n** coincide, the differential equations may be integrated in closed form to obtain (at the exit surface):

$$0°,\ \mu \neq 0,\quad P_H/P_0{}^\circ = \tfrac{1}{2}e^{-\mu T}(1-e^{-2\sigma T}), \tag{10}$$

$$\mu = 0,\quad P_H/P_0{}^\circ = \tfrac{1}{2}(1-e^{-2\sigma T}), \tag{11}$$

$$180°,\ \mu \neq 0,\quad P_H/P_0{}^\circ = \frac{\sigma \sinh (aT)}{a\cosh (aT)-\tau \sinh (aT)}$$

$$\text{with } a = (\tau^2-\sigma^2)^{\frac{1}{2}}, \tag{12}$$

$$\mu = 0,\quad P_H/P_0{}^\circ = \sigma T/(1+\sigma T), \tag{13}$$

where T is the path length through the crystal. For a cylindrical crystal with diameter D, we replace T by $D\cos\varphi$, integrate over φ, and, taking note of (9), obtain the following integrals for E_s:

$$0°,\ \mu \neq 0,\quad E_s = \frac{\int_0^{\pi/2} e^{-\mu D\cos\varphi}(1-e^{-2\sigma D\cos\varphi})\cos\varphi d\varphi}{2\sigma D\int_0^{\pi/2} e^{-\mu D\cos\varphi}\cos^2\varphi d\varphi}, \tag{14}$$

$$\mu = 0,\quad E_s = \frac{2}{\pi\sigma D}\int_0^{\pi/2}(1-e^{-2\sigma D\cos\varphi})\cos\varphi d\varphi, \tag{15}$$

$$180°,\ \mu \neq 0,$$

$$E_s = \frac{\int_0^{\pi/2} \dfrac{\sinh (aD\cos\varphi)\cos\varphi d\varphi}{a\cosh (aD\cos\varphi)-\tau\sinh (aD\cos\varphi)}}{\int_0^{\pi/2}\left(\dfrac{1-e^{-2\mu D\cos\varphi}}{2\mu}\right)\cos\varphi d\varphi}, \tag{16}$$

$$\mu = 0,\quad E_s = \frac{4}{\pi}\int_0^{\pi/2}\frac{\cos^2\varphi d\varphi}{1+\sigma D\cos\varphi}. \tag{17}$$

All the integrals appearing in (14)–(17) are conveniently evaluated by numerical methods. Integral (17) can also be evaluated in closed form. The following expansion is useful for some of the integrals:

$$\int_0^{\pi/2} e^{-b\cos\varphi}\cos\varphi d\varphi = J_0(ib)+\frac{i\pi}{2}J_1(ib)+\sum_{n=1}^{\infty}\frac{J_{2n}(ib)}{1-4n^2} \tag{18}$$

where $J_k(ib)$ is the Bessel function of order k of the pure imaginary argument ib. For very large and very small values of the parameters, certain of the expressions simplify. Table 1 presents values of the parameters for which the indicated approximations are valid to 2% or 5%. These expressions are readily verified by series expansion or sum approximations of the integrals in (14–(17).

Table 1. *Cylindrical crystal; approximate values of E_s with sufficient conditions for indicated error*

2θ	μ	E_s	Error < 2%	Error < 5%
0°	0	$2/\pi\sigma D$	$\sigma D > 7$	$\sigma D > 3$
0°	0	$\exp(-8\sigma D/3\pi)$	$\sigma D < 0{\cdot}3$	$\sigma D < 0{\cdot}5$
180°	0	$4/\pi\sigma D$	$\sigma D > 70$	$\sigma D > 30$
180°	0	$\exp(-8\sigma D/3\pi)$	$\sigma D < 0{\cdot}2$	$\sigma D < 0{\cdot}4$
180°	$\neq 0$	$2\mu/(a-\tau)$	$aD > 7$ $\mu D > 7$	$aD > 3$ $\mu D > 3$

Applications

For simplicity in presentation of results, we shall restrict ourselves in the following to examples with $\mu = 0$ ($\tau = -\sigma$); the calculations for non-vanishing μ are of course as easily carried out. The condition $\mu = 0$ is often applicable in neutron diffraction.

(a) Cylindrical crystals

Values of E_s for $2\theta = 0°$ and 180° were obtained as described immediately above, and values for $2\theta =$ 45°, 90°, and 135° were obtained by numerical integration over a grid. The mesh size chosen was such

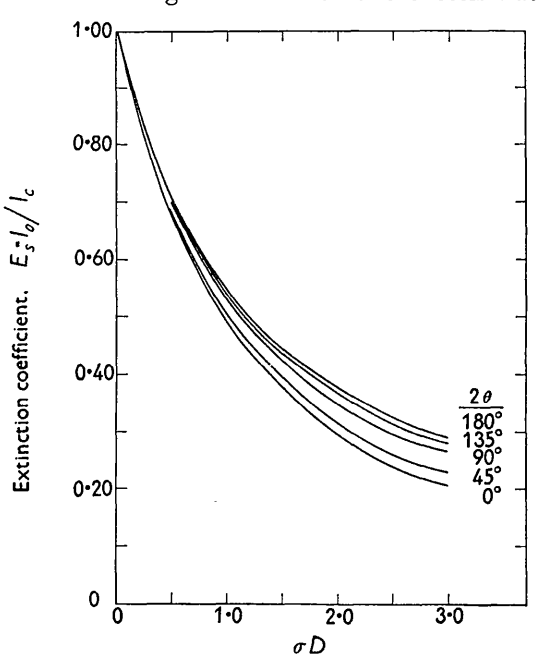

Fig. 3. Secondary extinction coefficient for cylindrical crystal at various Bragg angles plotted against $\sigma D = Q'DW(\Delta)$, where $W(\Delta) = 1/2\eta\sqrt{3}$ if $|\Delta| \leq \eta\sqrt{3}$ and $W(\Delta) = 0$ if $|\Delta| > \eta\sqrt{3}$. Error in E_s less than 3%.

that the maximum error in E_s is no greater than 3%. (The error is generally in the same direction for all points and of the same magnitude for points at different angles but similar σD.) The results for these five angles are plotted in Fig. 3. It is to be noted that the extinction coefficients of reflections at different Bragg angles vary by only about 3% at $\sigma D = 0{\cdot}50$ (corresponding to an E_s of approximately 0·7) but that the effect of angle becomes much more important at higher intensities. This is an important fact to keep in mind if one contemplates the application of empirical extinction corrections to observed reflections which are later to be used in a parameter refinement. In practice, one plots I_o versus I_c or I_o/I_c versus I_c to obtain an experimental E_s curve. The present results indicate that, for severe extinction, one obtains a different curve for every Bragg angle. Therefore, any empirical correction which is independent of Bragg angle can lead to large errors in E_s and consequently in the estimated true intensities of the more intense reflections. Fig. 4 indicates the range in possible

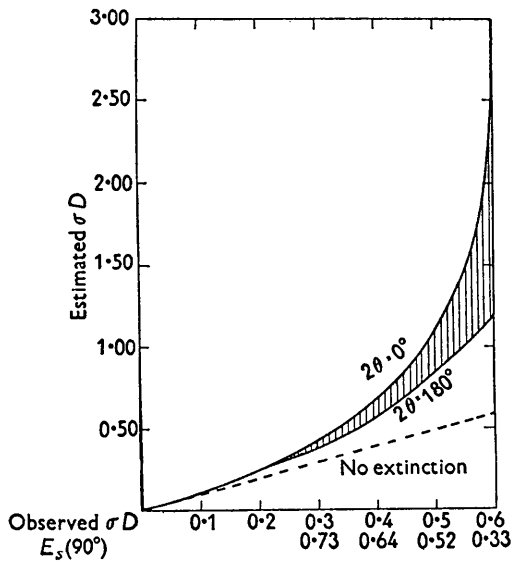

Fig. 4. Calculated versus observed intensities (intensity is proportional to σD^2) for the cylindrical specimen. Shaded region represents area of uncertainty in estimation of calculated intensity if Bragg angle of reflection is not taken into account.

estimated corrected intensities (corresponding to the range in E_s) as a function of the observed intensity. The corresponding E_s values at 90° are also indicated. The seriousness of this is realized when one notes that an estimate at the average value of the range may be about 50% in error for an E_s value of 0·30 and as great as 10% for an E_s value of 0·55, a situation which is not uncommonly encountered in neutron-diffraction experiments.

A further fact to keep in mind when dealing with intense reflections is that the observed intensities reach a limit as σD increases, i.e., they become no longer dependent on the value of F^2, but only on the size of the crystal, the mosaic spread, and the Bragg angle. This saturation phenomenon makes the estimation of the extinction correction subject to even further error. It is possible that one could make use of the limiting value of the intensity, if experimentally observed, to obtain an estimate of η which could then be used for the calculation of extinction corrections for the other reflections. These limiting values are, for the step function defined in (7) and no absorption,

$$\left.\begin{aligned} 180°: \quad R^{\theta}_{\text{lim.}} &= 2\sqrt{3}.hD\eta\,, \\ 0°: \quad R^{\theta}_{\text{lim.}} &= \sqrt{3}.hD\eta\,. \end{aligned}\right\} \tag{19}$$

This point was very nearly reached for the Fe_3O_4 crystal discussed below.

The above difficulties would seem to render inappropriate the use, in the ordinary way, of severely extinguished reflections in the deduction of an empirical extinction correction. Generally speaking, one has in any small range of 2θ too few reflections suffering from a high degree of extinction to permit the determination of reasonably accurate correction curves. A one-parameter extinction correction would be valid to 3% or better only when the extinction coefficient is greater than about 0·70. As noted in Table 1, in this range E_s may be approximated by

$$E_s = \exp\,(-8\sigma D/3\pi)\,. \tag{20}$$

(b) Rectangular crystals

The situation becomes much worse for crystals which do not have a circular cross-section, for E_s is then a function of crystal setting as well as of the Bragg angle. Fig. 5 shows this effect well for crystals

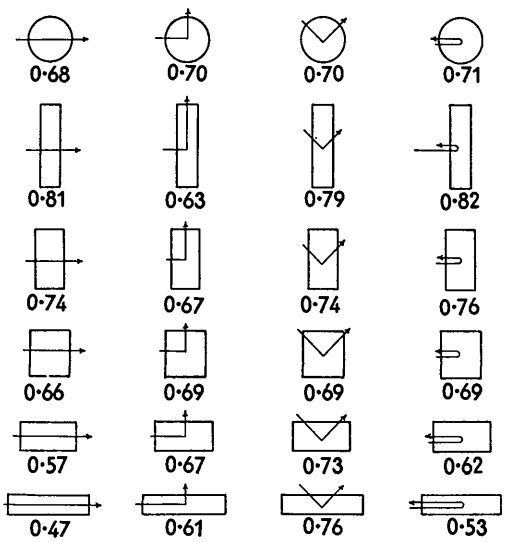

Fig. 5. Effect of crystal shape and setting on secondary extinction. All crystals have same cross-sectional area as cylinder with $D = 0{\cdot}50$. Rectangles have a/b ratios of $\frac{4}{1}$, $\frac{2}{1}$, $\frac{1}{1}$, $\frac{1}{2}$, and $\frac{1}{4}$. The arrows indicate the directions of incident and diffracted beams, and the numbers immediately below each crystal are the values of E_s.

of the same cross-sectional area as a cylinder with $\sigma D = 0{\cdot}50$, where, it will be recalled, the variation due to change in Bragg angle alone is about 3%. The values for a square pillar are close to those for a cylinder and show about the same angle variation. However, as the ratio of thickness to width departs from unity, the situation rapidly degenerates, the errors being, as expected, most dependent on crystal setting at very low and very high Bragg angles.

It would seem that if one wishes to make an empirical extinction correction with the most accuracy possible, the best procedure would be as follows:

(1) Use a cylindrical crystal.
(2) Determine a value for η from the less severely extinguished reflections (in the region where there is little dependence on Bragg angle: $E_s > 0{\cdot}70$) by applying equation (20) or its generalization to the case of finite absorption.
(2*a*) Alternatively, determine by equations (19) a value of η from the limiting intensities, if these are observed. It would be comforting if the two values checked.
(3) Using the η obtained from step (2) or (2*a*), use the calculated curves or suitable extensions of these to obtain extinction corrections for reflections in the intermediate range.

If other than equatorial reflections are to be measured, one would do better to employ a spherical crystal. E_s for such a crystal may be easily calculated from the corrections for a cylinder by numerical integration along a diameter of the sphere perpendicular to the sections, D in the above expressions now being taken to be the diameter of a circular slice at various depths in the crystal.

Experimental

We have recently measured by neutron diffraction the intensities of all (*hhl*) reflections with $\sin\theta/\lambda < 0{\cdot}88$ for a synthetic single crystal of Fe_3O_4 which shows particularly severe extinction. The crystal used is a pillar with a rectangular cross-section 1 mm. × 1·8 mm. perpendicular to the [110] axis. Absorption in the specimen was negligible. Application of equation (20) (taking D as 1·5 mm.) to the low-intensity data led to a mosaic spread parameter η of 11·5 sec. Fig. 6(*a*) is a plot of I_o versus I_c for all reflections with $I = F^2/\sin 2\theta < 100$ before and after the corresponding extinction correction was applied. The limiting intensity for reflections with 2θ near 90° seemed to be about 400. Assuming that the limiting value for 90° is the average of the limiting values for 0° and 180°. application of (19) gives a mosaic spread parameter of 13 sec. in excellent agreement with the value obtained from the low-intensity data. Fig. 6(*b*) is a log–log plot of I_o versus I_c for all reflections observed with $I > 10$, The curves are calculated for a cylinder of equivalent cross-sectional area with $\eta = 12$ sec. The agreement seems to be all that could be expected from the shape

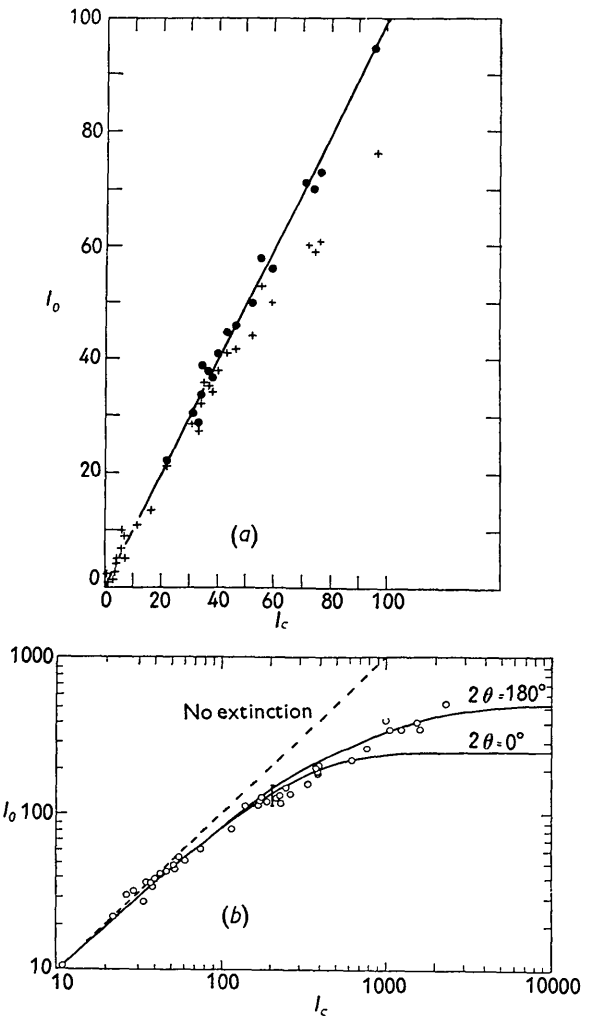

Fig. 6. Observed versus calculated intensities for (*hhl*) reflections of Fe_3O_4 single crystal of rectangular cross-section, 1 mm. × 1·8 mm. The straight lines represent perfect agreement.

(*a*) Low-intensity reflections. Crosses: raw observed intensities; dots: corrected by $E_s = \exp(-0{\cdot}0021 I_c)$.

(*b*) log–log plot of I_o versus I_c for all reflections. Curves are calculated for a cylindrical crystal with the same cross-sectional area as that of the real crystal and with a mosaic spread parameter η equal to 12 sec. The bar at $I_c = 200$ represents the additional spread in points which could arise because of the deviation of the crystal shape from that of the ideal cylinder.

of the crystal; the bar at $I_c = 200$ ($\sigma D = 0{\cdot}50$), for example, represents the additional variation which could come because of the departure of the crystal shape from the ideal cylinder. The limiting behavior at high intensities is clearly seen.

Because of the relatively small number of high intensity reflections, and because of the departure of the crystal shape from the ideal cylindrical form, no convincing smooth curves could be drawn for separate Bragg angles, although detailed calculations for a few of the reflections did agree qualitatively with the ex-

tinction ratios indicated in Fig. 5 for rectangles with an a/b ratio of 2/1.

It should be noted that several reflections with magnetic contributions are omitted from Figs. 6(a) and 6(b). These reflections had in every case intensities less than would be calculated from the curves which fit the pure nuclear peaks well. Consideration of the effect of beam polarization in conjunction with extinction effects indicates that this is precisely the behavior to be expected, and a detailed discussion of this will be the subject of a subsequent communication. This behavior will be observed in an unmagnetized crystal only if primary extinction is also present. One is thereby led to the conclusion that part of the extinction observed here is primary extinction, the amount of which is, however, somewhat less than the amount of secondary extinction. As the primary and secondary extinction curves are quite similar at low intensities, and as relatively few high-intensity reflections were observed, it is not surprising that a reasonable fit to the data was obtained by assuming that the extinction is entirely secondary extinction; however, the value of η derived is probably not a true mosaic-spread parameter but rather a parameter depending on both the mosaic spread and size of the mosaic blocks.

APPENDIX

(a) Absorption effects

In the above, we have treated numerically only examples with negligible true absorption. This is often quite adequate for neutron-diffraction work. Where absorption is important, one should calculate a set of extinction correction curves for the absorption coefficient characterizing the material with which one is working. It would not seem desirable at the present time to prepare tables covering a wide range in both σD and μD. As the absorption coefficient becomes larger, the importance of extinction becomes less. Fig. 7 illustrates the behavior at $2\theta = 180°$. It will be noted that for $\mu \gg \sigma$, E_s is approximately equal to $1-\sigma/\mu$ (compare Table 1).

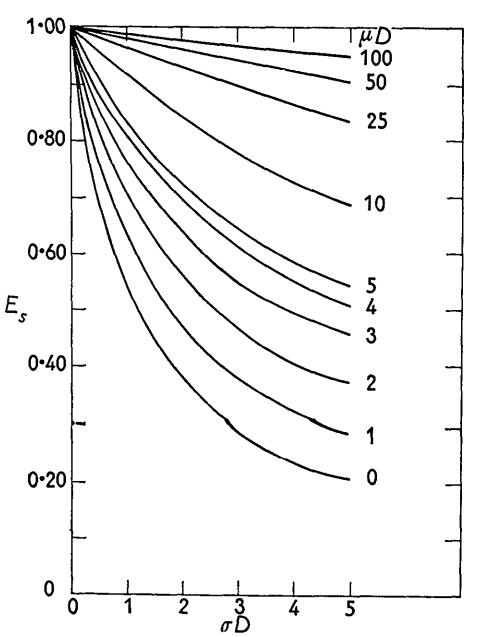

Fig. 7. Effect of absorption on the secondary extinction coefficient. Curves calculated for $2\theta = 180°$ and values of μD ranging from 0 to 100.

(b) Shape of the distribution function

The general effect of replacing the step distribution function $W(\Delta\theta)$ given in equation (7) by a Gaussian distribution function with the same standard deviation is indicated in Table 2. Although the values of E_s are significantly different for high intensities, the effects on the qualitative considerations of the previous sections are unimportant. Furthermore, even the quantitative effects can be largely accounted for by a simple change in scale of σD, i.e., the mosaic-spread parameter assigned in a particular case would depend on the shape of the distribution function assumed, but the general fit to the experimental data would be equally good in either case. As the one-parameter mosaic distribution is probably a rather inadequate description of the micro-structure of the crystal in any case, it would seem convenient to retain the simpler description of this form—the rectangular distribution function—for calculations of the type described in this paper. We have here derived expressions and curves in terms of $\sigma = QW(\Delta\theta)$, and, from these values, the values for any type of distribution function may be readily synthesized.

Table 2. *Extinction coefficients for cylinder as functions of shape of mosaic-distribution function, intensity, and Bragg angle*

		E_s for $Q'D/2\|/3.\eta =$		
2θ	$W(\Delta\theta)$	0·50	1·00	2·00
0°	Step	0·68	0·49	0·30
0°	Gaussian	0·69	0·52	0·34
180°	Step	0·71	0·55	0·38
180°	Gaussian	0·72	0·57	0·42

The author would like to express his appreciation to Drs J. M. Hastings and L. M. Corliss for stimulating his interest in this problem and for valuable criticism of the manuscript.

References

Bacon, G. E. (1955). *Neutron Diffraction*. Oxford: Clarendon Press.

Bacon, G. E. & Lowde, R. D. (1948). *Acta Cryst.* **1**, 303.

James, R. W. (1950). *The Optical Principles of the Diffraction of X-rays*. London: Bell.

Zachariasen, W. H. (1945). *Theory of X-ray Diffraction in Crystals*. New York: Wiley.